Hindawi
Advances in Civil Engineering
Volume 2021, Article ID 6797786, 10 pages
https://doi.org/10.1155/2021/6797786

Research Article

Desorption Characterization of Methane in Coal with Different Moisture Contents and Its Influence on Outburst Prediction

Peng Li,[1,2] Yaolin Cao,[1,2] Xuelong Li,[3,4] Fakai Wang,[5] Zhongguang Sun,[4,6] Deyou Chen,[3] Qinke Huang,[3] and Zhen Li[3]

[1]*China Coal Technology and Engineering Group Shenyang Research Institute Co., Ltd., Fushun, Liaoning 113122, China*
[2]*State Key Laboratory of Coal Mine Safety Technology, Fushun, Liaoning 113122, China*
[3]*College of Energy and Mining Engineering, Shandong University of Science and Technology, Qingdao, Shandong 266590, China*
[4]*State Key Laboratory of Coal Mine Disaster Dynamics and Control, College of Resources and Environmental Science, Chongqing University, Chongqing 400044, China*
[5]*College of Mining Engineering, Guizhou Institute of Technology, Guiyang 550000, China*
[6]*State Key Laboratory of The Gas Disaster Detecting, Preventing and Emergency Controlling, Chongqing 400037, China*

Correspondence should be addressed to Xuelong Li; lixlcumt@126.com

Received 30 August 2021; Accepted 1 December 2021; Published 21 December 2021

Academic Editor: Shun Liang

Coal and gas outburst is a dynamic phenomenon with violent eruptions of coal and gas from the working coal seam. It has been proved that rapid desorption within a short period is necessary for the occurrence of an outburst. Due to the limitation of the present test condition, gas desorption characterization in coal with different moisture content for the first several seconds (0–60 s) has not been researched sufficiently. In this study, initial desorption characterization of gas in coal with different moisture content is studied by experiments with methane. The most remarkable characteristic of the experimental setup is the application of a self-developed real-time data acquisition system with a time interval of about 10 ms, which achieves the goal of collecting enough pressure data for analysis and calculation. The data is used to study gas pressure variation and calculate the initial amount of desorbed gas and index (ΔP) of initial velocity diffusion of coal gas. From the experimental results, the new proof has been found to verify that coal with lower moisture content and methane outburst is more dangerous than coal with higher moisture content and outburst. The degree of coal and methane outburst is exponentially decaying with increasing moisture content.

1. Introduction

Gas is an associated product in the coal formation process [1]. Mine gas is deposited in coal beds in a few forms: (1) adsorbed in micropores and on the surface of larger pores, (2) absorbed in the coal molecular structure, (3) as free gas in fissures and larger pores whose share becomes of significance at higher sorbate pressures, and (4) dissolved in deposit waters [2–4]. Coal and gas outburst is a dynamic phenomenon with violent eruptions of coal and gas from the working coal seam, resulting in economic loss and casualties. It is becoming more and more serious as mining is extended deeper in seams [5, 6]. Coal and gas outburst accidents occur frequently during the process of uncovering coal in deep mines [7]. Many scholars have developed sensitivity indexes to predict outburst-prone coal seams through research on the desorption properties of coal [8, 9]. For instance, the variation K_V of gas emission was adopted to predict outburst proneness in Russia [10]. The gas emission V-index is a measure of the volume of gas desorption in the interval between 35 and 70 s in the condition of atmospheric pressure [11–13]. The gas adsorption index (K_1 and Δh_2) of drill cuttings has been conducted frequently in China. K_1 represents the volume of gas desorption in 1 min, and Δh_2 is the amount of gas desorption in the interval between 3 and 5 min under atmospheric pressure, respectively [14]. Moreover, the index (Δp) of initial velocity diffusion of coal gas has been widely adopted worldwide. Besides, time

constant T reflecting drop rate of gas pressure in front of the briquette face is proposed by Norbert [15].

These sensitivity indexes play a very important role in outburst prevention [16]. However, the effect of moisture on the gas desorption properties of coal particles is often overlooked during the experimental measurement process. Due to the fact that water in the coal will block the gas migration channel, thus blocking the gas desorption properties of coal particles and reducing the ability of coal diffusion [17–19], the study of moisture in the coal gas desorption characteristics is of great significance for the prevention and control of coal mine gas. A lot of research has been done. It was found that the diffusion rate of anthracite decreased with the increase of water content, while the diffusion rate of bituminous coal shows a U-shaped distribution with the increase of water content with decreases first and then increases [20]. Methane and carbon dioxide desorption diffusion experiments show that the moisture content in the coal matrix has a significant effect on the desorption rate of the gas, and the effect of moisture content on the diffusion rate of methane is greater than its effect on the diffusion rate of carbon dioxide [21, 22]. The results show that the initial desorption rate, diffusion capacity, and gas desorption capacity of coal are higher than those of static pressure after pulsating water injection, and the effect of gas desorption and diffusion is better than that of static pressure after water injection [23]. It is revealed that the gas desorption and desorption rates of the coal samples decrease with the increase of the moisture content of the coal samples in the same time period, regardless of the degree of metamorphism coal [24, 25]. The adsorption-water-desorption experiment was carried out to obtain the conclusion that the desorption rate decreased with the decrease of the critical pore scale [26]. The analysis of outburst prevention effect of coal seam water injection comes to the conclusion that the higher the original water content of the coal seam, the less the risk of coal and gas outbursts [27]. According to the study [28], it is shown that the cumulative gas removal rate of dry and wet coal samples is similar to that of Langmuir adsorption isotherm, and the addition of water restrains the coal desorption rate and the desorption rate of dry coal is larger than that of water.

In this paper, gas desorption characterization in the different moisture content for the first tens of seconds (0–60 s) is studied from three aspects: gas pressure, an initial amount of desorbed gas, and initial velocity diffusion of coal gas. Methane is used in the experiments. The effect of different moisture content on coal and gas outburst risk is analyzed. An effort is made to find a new proof for the phenomenon that coal and methane outburst with lower moisture content is more dangerous than that of higher moisture content.

2. Experimental Setup and Procedure

A schematic of the experimental setup is shown in Figure 1. It is mainly composed of a pressure container (5), a constant temperature water bath (11), a vacuum system (1), an inflation system (7–10), and a self-developed real-time data acquisition system (4). The container (5) is connected to the diffusion space (3) through the electromagnetic valve (6). A pressure regulating valve (8) is installed on the inflation system to achieve the designated gas pressure.

The application of the real-time data acquisition system is the most remarkable characteristic of the experimental setup. Time interval is brought down to about 10 ms to acquire enough gas pressure data in the initial desorption process. The ultimate pressure is almost decreasing to the level of an absolute vacuum (less than 10 mmHg). For the isovolumetric variable pressure measuring instrument, when the sample is not loaded, the diffusion space is degassed to make the pressure below 10 mmHg. After stopping the pump and placing it for 5 min, the increase of the space pressure should be less than 1 mmHg. Otherwise, the equipment should be overhauled until the airtightness meets the requirements.

Coal material was sampled from Quanlun coal mine of Shandong Energy Guizhou Co., Ltd., in Guizhou province, China. The geographical location of the Quanlun coal mine is shown in Figure 2. The to-be-mined coal seams in this coal mine are abundant, and the geological occurrence is simple, as shown in Figure 3. Pieces of coal were ground and sieved in order to achieve the desired size of 0.20 mm–0.25 mm. The weight of the coal sample was 3.5 grams. Proximate analysis of the coal sample was as follows: moisture content $M_{ad} = 1.50\%$, volatile matter content $V_{daf} = 7.06\%$, ash content $A_{ad} = 16.92\%$, total sulfur content $S_{t,d} = 0.56\%$, porosity $n = 10.49\%$, and average pore size $r = 9.3$ nm.

The coal sample was placed into the container (5). After 1.5 h evacuation, vacuum pump (1) was closed, while gas was injected into the container. So the coal sample adsorption was for 1.5 h. When the pressure remained constant, the electromagnetic valve (2) was opened, while electromagnetic valves (6, 7) were closed. The vacuum pump (1) was opened for degassing the diffusion space (including the instrument gas piping). Then, stop the vacuum pump, close the electromagnetic valve (2), and open the electromagnetic valve (6), so that the coal sample container and diffusion space are connected, and start the data acquisition. When the time is 10s, the electromagnetic valve (6) is closed and the diffusion space real-time pressure data are recorded. Then, when the time is 45s, the coal sample container and diffusion space are connected, and once again the diffusion space real-time is read.

When the coal sample container was filled with coal particles, methane was separately injected into the container. Experiments were carried out with equilibrium methane pressures of 0.100 MPa and moisture balance pretreatment content of 0.5%, 1%, 2%, 4%, 6%, 8%, and 10%. For comparison, the pressure regulating valve (8) was used to adjust the similar pressure under different gas conditions.

The following are the steps of moisture balance pretreatment of coal samples (as shown in Figure 4): First, weight a certain amount of air-dried coal sample (with a precision of 0.1 mg). Second, place the coal sample in a container and evenly add appropriate amount of distilled water. Third, place the container with the sample in a moisture-tight seal (25°C, a relative humidity of 97% in a humidified environment), which was filled with a sufficient

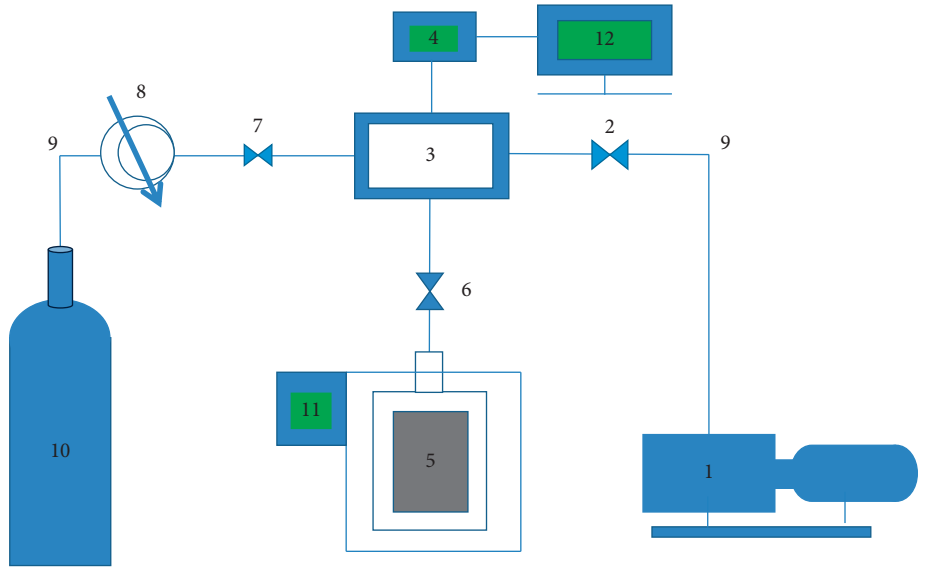

Figure 1: Schematic of the experimental setup. Denoted elements are 1, vacuum pump; 2, 6, and 7, electromagnetic valves; 3, diffusion space; 4, pressure transducer and real-time data acquisition system (DAS); 5, coal sample container; 8, pressure regulating valve; 9, gas piping; 10, gas cylinder; 11, constant temperature water bath; and 12, computer.

Figure 2: The geographical location of the Quanlun coal mine.

amount of potassium sulfate supersaturated solution and weight once every 24 hours until the two adjacent weight variations do not exceed 2% of the weight of the sample. The formula is as follows:

$$M_0 = \left(1 - \frac{G_2 - G_1}{G_2}\right) \times M_{ad} + \frac{G_2 - G_1}{G_2} \times 100, \quad (1)$$

where M_0 is moisture balance content of the sample, expressed as a percentage (%); G_1 is quality of the air-dried sample before balance, expressed in gram (g); G_2 is quality of the sample after balance, expressed in gram (g); M_{ad} is moisture content of the air-dried sample, expressed in percentage (%).

To eliminate the effect of the coal particles' own volume on the diffusion space, which is determined by their masses and densities, their masses were measured by using an analytical balance. The density of coal was measured by immersing in the paraffin method.

Since adsorption/desorption is extremely sensitive to temperature, the entire container was placed into the constant temperature water bath (11) with a water temperature of 25°C (298.15 K) during the whole experiments [29].

In order to ensure the reliability of the experimental setup, the airtightness of instrument needs to be detected. It was determined that the pressure change of the diffusion space in the test device is less than 10 Pa, which satisfied the pressure requirement of the coal gas dispersion process.

3. Results and Discussion

3.1. Initial Gas Pressure of Desorbed Gas. According to the measurement range of pressure transducer (0–0.100 MPa), data of real-time pressure data collected by pressure transducer and real-time data acquisition system is divided into two parts: the high range of 45 s pressure data ⟶ 60 s pressure data p_2 and the low range of 0 s pressure data ⟶10 s

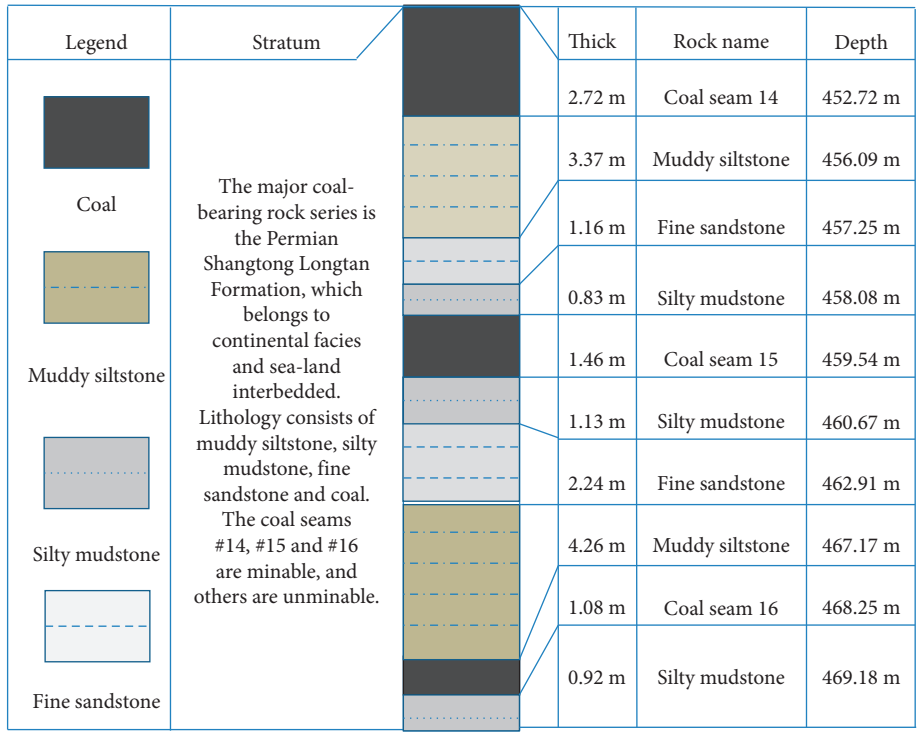

Figure 3: Coal seam histogram.

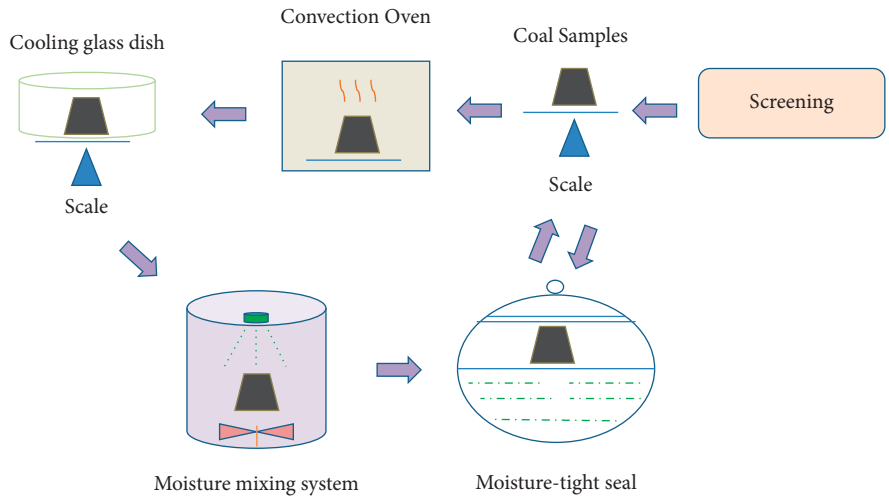

Figure 4: Schematic diagram of the preparation of coal samples and the moisture balance.

pressure data p_1 (p_1 is the first pressure data which is almost approximately equal to the 10 s diffusion space's pressure; p_2 is the last pressure data which is almost approximately equal to the 60 s diffusion space's pressure). To simplify data analysis, the 10 s–45 s inner coal sample container's pressure is discarded. The middle data (the 10 s–45 s diffusion space's pressure is constant) and pressure data collected by pressure transducer and real-time data acquisition system (0 s pressure data ⟶10 s pressure data; 45 s pressure data ⟶ 60 s pressure data) are combined for analysis. An example of pressure variation is shown in Figure 5.

It can be found that gas pressure increases sharply in the initial time and then levels slowly. Gas pressure variations are different in different time [30, 31]. The pressure rise rate of 45 s–60 s diffusion space's pressure is lower than that of 0 s–10 s diffusion space's pressure [32, 33]. The reason is that the adsorbed gas on micropore surfaces within the coal matrix is rapidly desorbed to free gas under the action of gas pressure gradient and concentration gradient [25–28].

The pressure variation when the container is filled with coal particles is shown in Figure 6. It can be found that the lower moisture content curve is always above the higher moisture content curve, which indicates that the diffusion

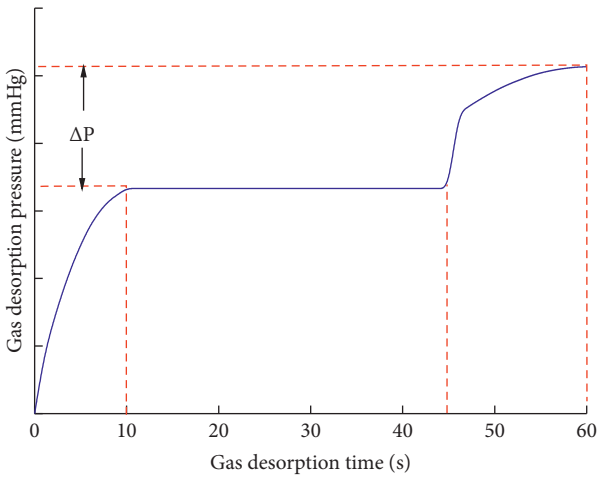

Figure 5: An example of pressure variation.

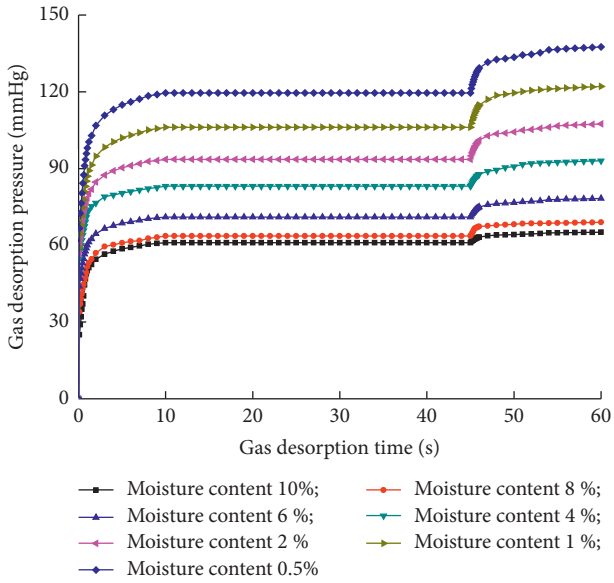

Figure 6: Pressure variation when the container is filled with coal particles.

space's pressure rise rate of methane in coal with higher moisture content is lower than that of lower moisture content [34]. That is to say, methane in coal with lower moisture content pressure keeps a high level for a longer time. Thus, a large amount of methane is desorbed to free gas after the exposure of coal, which contributes to producing enough energy for an outburst. The research result is consistent with the practical situation and laboratory experiments [20, 22].

3.2. Initial Amount of Desorbed Gas. The amount of gas diffusion (n) through the electromagnetic valve (6) consists of two parts: gas flux from the void volume (n_1) and that from the coal particles (n_2).

Collected data of gas desorption pressure is adopted to calculate gas mass flow (m) at the electromagnetic valve (6) by using [27]

$$m = \frac{P\sigma^*}{\sqrt{T}}\sqrt{\frac{2\gamma}{\gamma-1}\left[\left(\frac{P_2}{P}\right)^{2/\gamma} - \left(\frac{P_2}{P}\right)^{\gamma+1/\gamma}\right]}, \quad (2)$$

where p and T are the absolute pressure and temperature, respectively; p_2 is the atmospheric pressure; γ is the adiabatic exponent; σ^* is the cross-sectional area of the nozzle orifice; and R is the gas constant. The amount of gas flowing through the electromagnetic valve (6) can be calculated as

$$\begin{aligned} n &= \frac{1}{M}\int_0^{t_0} m\mathrm{d}t \\ &= \frac{PV}{298.15ZR}, \end{aligned} \quad (3)$$

where M is the molar mass of the gas; R is molar gas constant; V is the volume of the diffusion space; Z is the compressibility factor.

The calculation result is shown in Figure 7. It is evident from this figure that the total amount of desorbed gas is increasing with time at a great speed in the initial time. Then, the increasing rate continuously decreases.

From a microscopic view, the adsorption of water and methane in coal is due to the interaction of water molecules and methane molecules with coal-based molecules [35, 36]. The maximum adsorption potential of methane on the coal surface is −2.704 kJ/mol, and the maximum adsorption potential of water on the coal surface is −24.0 k/mol. The larger the adsorption potential is, the more adsorbable molecules are adsorbed [35–38]. Therefore, the water in coal has a great influence on the adsorption capacity of methane. Water mainly affects the adsorption of coal to gas through three aspects [37–40]: First, the combination of partial free water and coal surface occupies a certain coal surface space, thus reducing the adsorption space of methane molecules and reducing the adsorption of methane on the coal surface. Second, because the water has a certain vapor pressure, a small amount of water molecules in gaseous form exists in coal micropore, hindering the methane molecules adsorbed in the coal surface and reducing the amount of methane absorbed by coal. Third, water blocks the channel of methane molecules into the micropores. Due to the fact that the specific surface area of the pores is the main carrier of coal adsorption [41], water will form capillary resistance within the micropores of coal [42, 43]. Especially when the pressure between the internal and the external environments of the pores is insufficient to overcome the capillary resistance, the methane molecules are prevented from entering the pores, thereby reducing the amount of adsorbed methane in coal [44]. In general, water reduces the amount of adsorbed gas in the coal sample, thereby reducing the initial desorption pressure of the gas.

Gas flux from the container volume (n_1) is equal to the gas increase in the diffusion space volume, and it can be calculated as

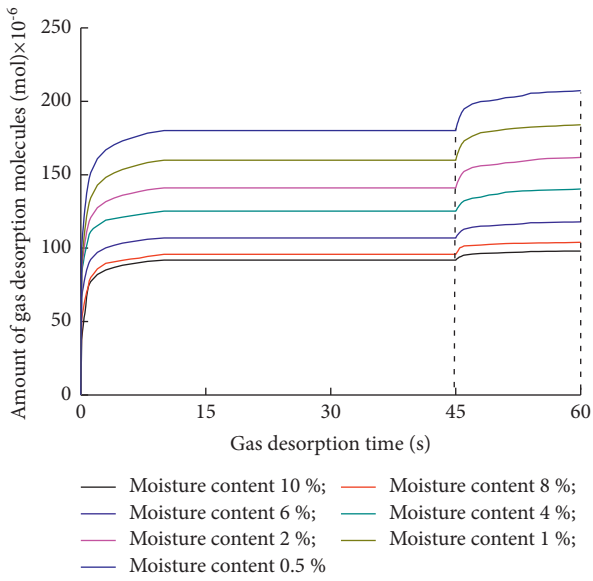

Figure 7: The relation between the total amount of gas desorbed from the coal particles and time.

$$\Delta n = \frac{V}{298.15R}\left(\frac{P_2}{Z_2} - \frac{P_1}{Z_1}\right), \tag{4}$$

where p_1 and p_2 are the absolute pressures; V is the volume of the diffusion space; Z is the compressibility factor. The velocity of gas desorbed from coal particles (v) in unit time Δt is calculated as

$$v = \frac{\Delta n}{\Delta t}. \tag{5}$$

The calculation result is shown in Figure 8. It is evident from this figure that the desorbed gas velocity is decreasing with time at a great speed in the initial time. Then, the decreasing rate continuously decreases. The trend lines have an unstable fluctuation curve in the time of 0.4–1.2 s; and they are similar in the time of 45–49 s at the same moisture content. For the data of experiments at the moisture content level of 10%, the desorbed gas velocity is slightly larger than that after the unstable fluctuation curve. Then, the total amount of desorbed methane is still increasing fast. With the time increasing, the total desorbed gas gap between the time period of 0–10 s and the time period of 45–60 s is larger and larger. They are similar at the other moisture content levels.

3.3. Initial Velocity Diffusion of Coal Gas. The index (ΔP) of initial velocity diffusion of coal gas (abbreviated as IVDCG) is an index that is used widely worldwide to identify outburst-prone coal seams. It has been proved that the occurrence probability of outburst increases with the increase of IVDCG and the threshold for outburst coal seams is 10 mmHg, respectively.

According to the research of Yang and Wang [45], when the coal particle size is less than the limit size, the coal particles are basically composed of pore structure. The limit particle size varies with the coal, about 0.5–10 mm [46]. Therefore, the mass flow of gas at the initial velocity measurement will be proportional to the gas concentration gradient, which is consistent with the diffusion law, that is, the law of Fick.

$$J = -D\frac{\partial C}{\partial X}, \tag{6}$$

where J is the diffusion velocity, $m^3/(m^2 \cdot s)$; D is the coal gas diffusion coefficient, m^2/s; C is the coal gas concentration, m^3/t; X is the distance from the center of the particle, m.

A large number of experiments at home and abroad show that when the coal adsorbs gas, the adsorption isotherms conform to the Langmuir equation [47, 48]:

$$W = \frac{abP}{1+bP} \times \frac{1}{1+0.31M_0}, \tag{7}$$

where W is at a certain temperature, when the adsorption equilibrium gas pressure is p, mL/g; P is gas pressure at adsorption equilibrium, MPa; a is the adsorption constant, which is the maximum amount of adsorbed gas, mL/g, when the gas pressure approaches infinity at a certain temperature; b is adsorption constant, MPa^{-1}, b is the reciprocal of Langmuir pressure; M_0 is moisture balance content of the sample, %.

Suppose the following: (1) the coal dust is composed of spherical particles; (2) the coal is homogeneous and the same; (3) the gas flow conforms to the law an of conservation of mass and the continuity principle; (4) the average radius R of the coal particles is 0.125 mm.

Coal particles desorption coalbed methane in the first-class boundary conditions of the approximate solution [49] is as follows:

$$\frac{C - C_P}{C_0 - C_P} = -\frac{2R(-1)^n}{\pi r n}\sin\frac{n\pi r}{R}\exp\left(-n^2\pi^2\frac{Dt}{R^2}\right). \tag{8}$$

According to the determination method for index Δp, the following can be obtained:

$$\Delta P = \frac{3.5}{27\rho\left(4/3\pi R^3\right)}\int_0^{60}\left(\iiint_V (C_0 - C_P)\mathrm{d}V\right)\mathrm{d}t, \tag{9}$$

where ρ is coal particle density; C_P is a gas concentration at any time.

The approximate solution of the index Δp is obtained by formulas (8) and (9):

$$\Delta P = \frac{3.5}{27\rho}\left(\frac{abP}{1+bP} \times \frac{1}{1+0.31M_0} - C_P\right)\left\{\sum_{n=1}^{\infty}\frac{6}{\pi^2 n^2}\left[\exp\left(-\pi^2 n^2\frac{60D}{R^2}\right) - \exp\left(\pi^2 n^2\frac{10D}{R^2}\right)\right]\right\}. \tag{10}$$

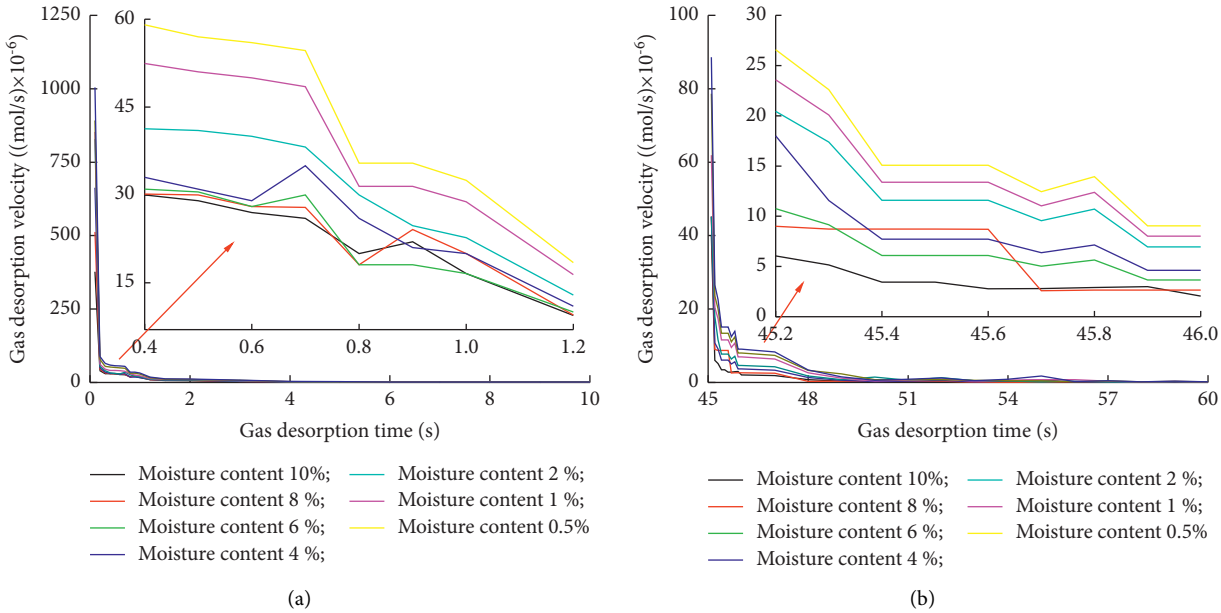

Figure 8: The relation between gas desorbed velocity from the coal particles and time. (a) Time range of 0 s–10 s. (b) Time range of 45 s–60 s.

From formula (10), moisture content on the determination of a greater impact can be obtained. Regardless of the effect of adsorption temperature and adsorption pressure, the gas diffusion coefficient D of the coal is constant, so different coal samples are affected by the moisture content. The greater the amount of gas adsorption, the greater the effect of the moisture content on the IVDCG. Under conditions of constant equilibrium gas adsorption pressure and the same coal sample, the lower the moisture content, the greater the index Δp; the higher the moisture content, the smaller the index Δp. In addition, the IVDCG and the adsorption constants of coal have a certain relationship. According to the IVDCG, the ultimate adsorption capacity of coal can be estimated.

The measurement result is presented in Table 1, which has shown that the moisture content has a dramatic influence on the measuring of IVDCG, and the larger moisture content in the uniform coal is, the smaller the IVDCG will be. To investigate the variation of IVDCG with moisture content, the measured IVDCG with various moisture contents has been regressively analyzed.

The regression analysis results are presented in Table 2. The regression analysis results have shown that R-squared of an exponential function is the largest, so the IVDCG is exponentially reducing, while the water content of the coal sample is increasing. It can be seen from Figure 9 that when the equilibrium moisture content is subjoined by 9.5%, the reduction rate of the index Δp (methane) is 34.9%. So we got that the IVDCG is greatly affected by the moisture content. With the increase of equilibrium moisture content, the IVDCG decrease is reducing. It can be seen that the data show that the IVDCG is greatly influenced by the equilibrium moisture content.

The relationship between IVDCG and equilibrium moisture content is shown in Figure 9. References [31–33] have proved that IVDCG varies directly with moisture. However, there is no experimental result for coal containing moisture content. From Figure 9, it is found that the relationship is adequately described by the exponential function equation of $\Delta p = k \exp(-A^* M_{ad}) + B$ (k is the coefficient of moisture influence, the value of which indicates the degree of moisture affecting the IVDCG; A is the attenuation coefficient of the IVDCG, and its value indicates the effect of moisture on the rate of decrease of the IVDCG; B is the constant).

According to the outburst threshold of 10 mmHg (as is shown in Table 3) [11], coal seams should be identified as non-outburst-prone seams when the moisture content is higher than 4% for the experimental coal sample in the adsorption methane pressure 0.1 MPa condition, which confirms that the lower moisture content coal and methane outburst is more dangerous than that of higher moisture content.

Also, the IVDCG (Δp) and the adsorption constants (a and b value) of coal have a certain relationship [50]. Therefore, the ultimate adsorption capacity of coal can be estimated approximately according to the initial speed of gas diffusion.

The index ΔP is an indicator of the capacity of coal to adsorb gas at standard atmospheric pressure (0.1 MPa) and the speed of gas desorption when exposed to air suddenly. The performance of coal to diffuse gas is determined by the physical and mechanical properties of coal. Under the same moisture content, the greater the IVDCG, the greater the risk of coal and gas outburst [51].

The index ΔP is one of the indicators used for the coal and gas outburst forecast, the critical value of which is 10 mmHg. When $\Delta p \geq 10$ mmHg, the coal seam has the outburst risk; when $\Delta p < 10$ mmHg, the coal seam does not have the outburst risk.

Table 1: Index Δp measurement results.

CH_4	M_{ad} (%)	0.5	1	2	4	6	8	10
	Δp (mmHg)	17.9	15.8	13.8	10.0	7.3	5.4	4.1

Table 2: The regression analysis results.

Model	Fitting formula	Adj. R-squared
Linear	$\Delta p = 17.07–1.43^{*} M_{ad}$	0.9464
Exponential	$\Delta p = 18.07^{*}\exp(-M_{ad}/5.6) + 1.08$	0.9978
Logarithmic	$\Delta p = 15.66–4.68^{*}\ln(M_{ad})$	0.9735
Power	$\Delta p = 15.59^{*} M_{ad}^{-0.47}$	0.8953

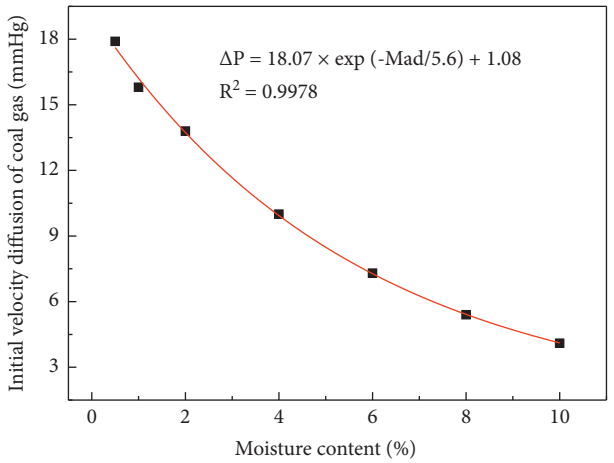

Figure 9: The relationship between IVDCG and equilibrium moisture content.

Table 3: Indicator thresholds.

Coal seam	Initial velocity diffusion of coal gas (Δp)	Initial velocity diffusion of coal gas (Δp)
The critical value	≥10	<10
Outburst risk	Danger	Safe

According to the obtained exponential function equation, it can be seen that, with the increase of the moisture content of coal samples, the index Δp of IVDCG has exponential decrease. In particular, the experimental result shows that when the moisture content of coal samples increased to more than 4%, the index Δp of IVDCG will be reduced to below the critical value of 10 mmHg. It can be seen that, in the case of coal samples which used water injection measures to determine the IVDCG, as the coal sample moisture increased, it makes the index Δp of IVDCG decrease, thus covering the information of coal and gas outburst risk, which will cause actual inconsistent results.

Due to the small amount of data in this experiment, the problem of correction will continue in the future study.

4. Conclusions

(1) The greater the amount of gas adsorption, the greater the effect of the moisture content on the IVDCG. Under conditions of constant equilibrium gas adsorption pressure and the same coal sample, the lower the moisture content, the greater the index Δp; the higher the moisture content, the smaller the index Δp.

(2) The desorbed gas velocity is decreasing with time at a great speed in the initial time. Then, the decreasing rate continuously decreases. For the data of experiments at the moisture content level of 10%, the desorbed gas velocity is slightly larger than that after the unstable fluctuation curve. Then, the total amount of desorbed methane is still increasing fast. With the time increasing, the total desorbed gas gap between the time period of 0–10 s and the time period of 45–60 s is larger and larger.

(3) IVDCG is greatly affected by the moisture content. The relationship between IVDCG and equilibrium moisture content is adequately described by the exponential function equation of $\Delta p = k\, e^{-A\mathrm{Mad}} + B$. With the increase of equilibrium moisture content, the index Δp has exponential decrease.

(4) When the moisture content of coal samples increased to more than 4%, the index Δp of IVDCG will be reduced to below the critical value of 10 mmHg; thus coal seams should be identified as non-outburst-prone seams in the adsorption methane pressure 0.1 MPa condition.

(5) Determination index Δp should try to keep the coal samples moisture content consistent with that of the site coal seam. If the critical value (10 mmHg) is used, it should be adjusted according to the actual moisture content of the coal seam after water injection.

Data Availability

The data used to support the findings of this study are available from the corresponding author upon request.

Conflicts of Interest

The authors declare that they have no conflicts of interest.

Acknowledgments

This work was financially supported by the National Natural Science Foundation of China (52104204), the cultivation and exploration and innovation project of new academic seedlings of Guizhou Institute of Technology (GZLGXM-04), the Natural Science Foundation of Chongqing, China (cstc2019jcyj-msxmX0633, cstc2019jcyj-bsh0041, and cstc2020jcyj-msxmX0972), Natural Science Foundation of Shandong Province (ZR2021QE170), the Science Innovation and Entrepreneurship Special Funded Projects of China Coal Technology & Engineering Group (2020-TD-ZD007), and the Science and Technology Planning Project of

Jiulongpo District (2020-02-005-Y), which are gratefully acknowledged.

References

[1] A. Tahmasebi, J. Yu, Y. Han, and X. Li, "A study of chemical structure changes of Chinese lignite during fluidized-bed drying in nitrogen and air," *Fuel Processing Technology*, vol. 101, pp. 85–93, 2012.

[2] K. Kotarska, W. Dziemianowicz, and A. Wierczyńska, "The effect of detoxification of lignocellulosic biomass for enhanced methane production," *Energies*, vol. 14, no. 18, pp. 1–14, 2021.

[3] Y. Fu, X. Liu, B. Ge, and Z. Liu, "Role of chemical structures in coalbed methane adsorption for anthracites and bituminous coals," *Adsorption*, vol. 23, no. 5, pp. 711–721, 2017.

[4] U. Hee, V. Lee, and Z. Semenovich, "About possibilities to improve current outburst hazard prediction based on updated mechanism of coal and gas outburst," *Mining Report*, vol. 152, no. 2, pp. 161–170, 2016.

[5] B. B. Beamish and P. J. Crosdale, "Instantaneous outbursts in underground coal mines: an overview and association with coal t, ype," *International Journal of Coal Geology*, vol. 35, no. 1-4, pp. 27–55, 1998.

[6] A. Fisne and O. Esen, "Coal and gas outburst hazard in Zonguldak Coal Basin of Turkey, and association with geological parameters," *Natural Hazards*, vol. 74, no. 3, pp. 1363–1390, 2014.

[7] X. Li, Z. Cao, and Y. Xu, "Characteristics and trends of coal mine safety development," *Energy Sources, Part A: Recovery, Utilization, and Environmental Effects*, pp. 1–19, 2020.

[8] Z. Zhang, X. Liu, Y. Zhang, X. Qin, and M. Khan, "Comparative study on fracture characteristics of coal and rock samples based on acoustic emission technology," *Theoretical and Applied Fracture Mechanics*, vol. 111, Article ID 102851, 2021.

[9] C. Wang, D. Song, C. Zhang, L. Liu, Z. Zhou, and X. Huang, "Research on the classification model of coal's bursting liability based on database with large samples," *Arabian Journal of Geosciences*, vol. 12, no. 13, p. 411, 2019.

[10] H. Wang, E. Wang, and Z. Li, "Study on dynamic prediction model of gas emission in tunneling working face," *Combustion Science and Technology*, vol. 6, pp. 1–17, 2020.

[11] M. Ochowiak, S. Woziwodzki, M. Doligalski, M. Micha, and T. Piotr, "[Lecture notes on multidisciplinary industrial engineering] practical aspects of chemical engineering || superheated steam drying of solid fuels: wood biomass and lignite," *Practical Aspects of Chemical Engineering*, vol. 25, pp. 363–375, 2018.

[12] S. M. Mezghanni, *Étude de la fiabilité des communications dans un réseau de capteurs sans-fils appliqué aux mines souterraines*, Depositum, Paris, France, in French, 2018.

[13] R. Dhuot, "La genèse précoce des différences sociales dans les habitudes alimentaires," *Research Gate*, vol. 15, Article ID 02069319, 2018.

[14] National Mine Safety Administration, *Regulation of Coal and Gas Outburst Prevention and Control*, China coal industry publishing home, Beijing, China, 2019.

[15] S. Norbert, A. Pajdak, K. Kozie, and T. Leticia, "Methane emission during gas and rock outburst on the basis of the unipore model," *Energies*, vol. 12, no. 10, pp. 1–22, 2019.

[16] X. Li, S. Chen, E. Wang, and Z. Li, "Rockburst mechanism in coal rock with structural surface and the microseismic (MS) and electromagnetic radiation (EMR) response," *Engineering Failure Analysis*, vol. 124, Article ID 105396, 2021.

[17] Y. Zhou, H. Li, J. Huang et al., "Influence of coal deformation on the Knudsen number of gas flow in coal seams," *Energy*, vol. 233, Article ID 121161, 2021.

[18] M. Pillalamarry, S. Harpalani, and S. Liu, "Gas diffusion behavior of coal and its impact on production from coalbed methane reservoirs," *International Journal of Coal Geology*, vol. 86, no. 4, pp. 342–348, 2011.

[19] E. S. Alias, M. Mukhtar, and R. Jenal, "Instrument development for measuring the acceptance of UC&C: a content validity study," *International Journal of Advanced Computer Science and Applications*, vol. 10, no. 4, pp. 187–193, 2019.

[20] D. Wu, Y. Zhao, Y. Cheng, and F. An, "ΔP index with different gas compositions for instantaneous outburst prediction in coal mines," *Mining Science and Technology (China)*, vol. 20, no. 5, pp. 723–726, 2010.

[21] Y. Zhou, Z. Li, R. Zhang et al., "CO2 injection in coal: advantages and influences of temperature and pressure," *Fuel*, vol. 236, pp. 493–500, 2019.

[22] J. Sobczyk, "A comparison of the influence of adsorbed gases on gas stresses leading to coal and gas outburst," *Fuel*, vol. 115, pp. 288–294, 2014.

[23] M.-y. Chen, Y.-p. Cheng, H.-r. Li, L. Wang, K. Jin, and J. Dong, "Impact of inherent moisture on the methane adsorption characteristics of coals with various degrees of metamorphism," *Journal of Natural Gas Science and Engineering*, vol. 55, pp. 312–320, 2018.

[24] Q. Zou, B. Lin, C. Zheng et al., "integrated techniques of drilling–slotting–separation-sealing for enhanced coal bed methane recovery in underground coal mines," *Journal of Natural Gas Science and Engineering*, vol. 26, pp. 960–973, 2015.

[25] J. Cordeiro, A. L. Magalhães, A. A. Valente, and C. M. Silva, "Experimental and theoretical analysis of the diffusion behavior of chromium(III) acetylacetonate in supercritical CO_2," *The Journal of Supercritical Fluids*, vol. 118, pp. 153–162, 2016.

[26] X. Du, Y. Cheng, Z. Liu et al., "CO_2 and CH_4 adsorption on different rank coals: a thermodynamics study of surface potential, Gibbs free energy change and entropy loss," *Fuel*, vol. 283, Article ID 118886, 2021.

[27] L. Xu, C. Jiang, and S. Tian, "Experimental study of the gas concentration boundary condition for diffusion through the coal particle," *Journal of Nature Gas Science & Engineering*, vol. 21, pp. 451–455, 2014.

[28] S. Wang, D. Elsworth, and J. Liu, "Rapid decompression and desorption induced energetic failure in coal," *Journal of Rock Mechanics & Geotechnical Engineering*, vol. 7, pp. 345–350, 2015.

[29] S. Liu, X. Li, D. Wang, and D. Zhang, "Experimental study on temperature response of different ranks of coal to liquid nitrogen soaking," *Natural Resources Research*, vol. 32, pp. 1467–1480, 2021.

[30] Z. Zhang, E. Wang, X. Liu et al., "Anisotropic characteristics of ultrasonic transmission velocities and stress inversion during uniaxial compression process," *Journal of Applied Geophysics*, vol. 186, Article ID 104274, 2021.

[31] X. Kong, S. Li, E. Wang et al., "Dynamics behaviour of gas-bearing coal subjected to SHPB tests," *Composite Structures*, vol. 256, Article ID 113088, 2021.

[32] X. Li, S. Chen, Q. Zhang, X. Gao, and F. Feng, "Research on theory, simulation and measurement of stress behavior under regenerated roof condition," *Geomechanics and Engineering*, vol. 26, pp. 49–61, 2021.

[33] X. Li, S. Chen, S. Liu, and Z. Li, "AE waveform characteristics of rock mass under uniaxial loading based on Hilbert-Huang transform," *Journal of Central South University*, vol. 28, pp. 1843–1856, 2021.

[34] X. Kong, S. Li, E. Wang et al., "Experimental and numerical investigations on dynamic mechanical responses and failure process of gas-bearing coal under impact load," *Soil Dynamics and Earthquake Engineering*, vol. 142, Article ID 106579, 2021.

[35] H. Mu, Y. Bao, D. Song, and D. Su, "Investigation of strong strata behaviors in the close-distance multiseam coal pillar mining," *Shock and Vibration*, vol. 9, pp. 1–14, 2021.

[36] J. Zang, K. Wang, and Y. Yu, "Effects of particle size on diffusion kinetics in Chinese anthracites during CH_4 desorption," *Processes*, vol. 8, no. 5, 2020.

[37] Z. J. Pan, L. D. Connell, M. Camilleri, and C. Leo, "Effects of matrix moisture on gas diffusion and flow in coal," *Fuel*, vol. 89, no. 11, pp. 3207–3217, 2010.

[38] J. Xie, J. Xie, G. Ni, R. Sheik, Q. Sun, and H. Wang, "Effects of pulse wave on the variation of coal pore structure in pulsating hydraulic fracturing process of coal seam," *Fuel*, vol. 264, Article ID 116906, 2020.

[39] F. Wang, X. Li, B. Cui et al., "Experimental study on adsorption promotion and desorption restrain of gas-containing coal in low-temperature environment," *Arabian Journal of Geosciences*, vol. 14, no. 12, pp. 1–12, 2021.

[40] J. Jiang, Y. Cheng, J. Mou, and K. Jin, "Effect of water invasion on outburst predictive index of low rank coals in dalong mine," *Plos One*, vol. 10, no. 7, Article ID e0132355, 2015.

[41] S. Alexander and D. Yuliya, "Geophysical criterion of pre-outburst coal outsqueezing from the face space into the working," *International Journal of Mining Science and Technology*, vol. 29, no. 3, pp. 152–159, 2019.

[42] H. Wang, Y. Tao, D. Wang, and X. Sin, "Experimental study on mechanical properties of briquette coal samples with different moisture content," *Geofluids*, vol. 2021, Article ID 6634378, 11 pages, 2021.

[43] K. Yamakawa and K. Fukutani, "Nuclear spin conversion of H_2, H_2O, and CH_4 interacting with diamagnetic insulators," *Journal of the Physical Society of Japan*, vol. 89, no. 5, Article ID 051016, 2020.

[44] Q. Zou, H. Liu, Z. Jiang, and X. Wu, "Gas flow laws in coal subjected to hydraulic slotting and a prediction model for its permeability-enhancing effect," *Energy Sources, Part A: Recovery, Utilization, and Environmental Effects*, vol. 75, 2021.

[45] Y. Yang and S. Liu, "Estimation and modeling of pressure-dependent gas diffusion coefficient for coal: a fractal theory-based approach," *Fuel*, vol. 253, pp. 588–606, 2019.

[46] Y. Liang, F. Wang, X. Li, C. Jiang, L. Li, and Y. Chen, "Study on the influence factors of the initial expansion energy of released gas," *Process Safety & Environmental Protection*, vol. 117, pp. 582–592, 2018.

[47] B. Guo, Y. Li, F. Jiao, T. Luo, and Q. Ma, "Experimental study on coal and gas outburst and the variation characteristics of gas pressure," *Geomechanics and Geophysics for Geo-Energy and Geo-Resources*, vol. 4, pp. 355–368, 2018.

[48] C. Wang, S. Yang, J. Li, X. Li, and C. Jiang, "Influence of coal moisture on initial gas desorption and gas-release energy characteristics," *Fuel*, vol. 232, pp. 351–361, 2018.

[49] Z. Wang, X. Tang, G. Yue, and B. Kang, "Physical simulation of temperature influence on methane sorption and kinetics in coal: benefits of temperature under 273.15 K," *Fuel*, vol. 158, pp. 207–216, 2015.

[50] B. Nie, X. Liu, L. Yang, and J. Meng, "Pore structure characterization of different rank coals using gas adsorption and scanning electron microscopy," *Fuel*, vol. 158, pp. 908–917, 2015.

[51] K. Jin, Y. Cheng, T. Ren et al., "Experimental investigation on the formation and transport mechanism of outburst coal - gas flow: implications for the role of gas desorption in the development stage of outburst," *International Journal of Coal Geology*, vol. 194, pp. 45–58, 2018.

[52] H. Zhu, Y. Zhang, S. Fang, and Y. Huo, "Methane adsorption influence and diffusion behavior of coking coal macromolecules under different moisture contents," *Energy & Fuels*, vol. 34, no. 12, p. 15920, 2020.

[53] H. Ullah, G. Liu, B. Yousaf et al., "Hydrothermal dewatering of low-rank coals: influence on the properties and combustion characteristics of the solid products," *Energy*, vol. 158, pp. 1192–1203, 2018.